J. Fluid Mech. (1964), *vol.* 20, *part* 3, *pp.* 447–455
Printed in Great Britain

The 'piston problem' with thermal radiation

By KUO CHANG WANG
The Martin Company, Baltimore, Maryland

(Received 27 December 1963 and in revised form 26 May 1964)

The classical problem of the motion of a one-dimensional unsteady shock generated by a piston moving with velocity $v_p = ct^n$ is extended to take into account thermal radiation effects by the similarity method of Taylor and Sedov. Gray gas and local thermodynamic equilibrium are assumed and a modification of the Schuster–Schwarzschild differential equation for the heat flux is adopted. The optical thickness is not restricted to be thin or thick, and the absorption coefficient is assumed to vary with the density and temperature. Numerical results indicate that the pressure and velocity are not affected much by the radiation, but the density, temperature and radiant heat flux are changed considerably.

1. Introduction

As a result of increasing flight speeds in space exploration, thermal radiation becomes increasingly more important in aerodynamic problems. In the present work, we shall extend the one-dimensional 'piston problem' considered by Taylor (1946) and Sedov (1959) to take into account radiation.

Previous investigations by Marshak (1958) and Elliott (1960) on one-dimensional unsteady radiating shock motion are all limited to the optically thick case. Part of Elliott's work is, in fact, very similar to an earlier one of Korobeinikov (1957). More recently, Trilling (1963), using the method of separation of variables, obtained similar solutions of a Cauchy-type one-dimensional unsteady problem with radiation effects; but the absorption coefficient was assumed to be some average constant.

In the present work, both the limitation of thick opacity and constant absorption coefficient are removed. Of course, certain common simplifications are still necessary in order to make the problem less complicated. These include: local thermodynamic equilibrium, gray gas, transparent shock, black and cool piston, perfect gas, and negligible radiation pressure and energy.

Two different approaches have been widely used in radiation gas dynamics. One is the integro-differential approach; the other the differential approach. For ease in obtaining similar solutions, the differential approach was chosen for this work. In many one-dimensional radiative transfer problems, including the one considered here, the boundary conditions are specified in terms of q_{r+} and q_{r-}, the average heat flux along two opposite directions in a one-dimensional problem. It is therefore more convenient to deal with two first-order differential equations for q_{r+} and q_{r-}. In classical astrophysics literature, this is known as the

Schuster–Schwarzschild method (cf. Sobolev 1963). Actually, the differential equations used here are a modified version of Schuster–Schwarzschild's original ones recently suggested by Traugott & Wang (1964). The differential method yields results in excellent agreement with the exact integro-differential method, at least for some problems (cf. Adrianov & Polyak 1963).

Two similarity conditions due to radiation are first determined; the system of partial differential equations is then reduced to one of ordinary differential equations. The latter is numerically integrated for various cases, but all the results reveal similar trends of the radiation effects. It is found that radiation has practically no effect on pressure and velocity, increases the density (hence lowers the temperature) considerably, and decreases the shock distances until a minimum value is reached.

The background of the piston problem has been well explored (Sedov 1959; Kochina & Mel'nikova 1958). Results of the present work may find direct application to problems such as stagnation-point flow, explosion, shock-tube flow, and hypersonic flow over slender power-law bodies (restricted to the thin or thick limit in order that the gas slabs normal to the body axis are independent of each other). Meanwhile, the present results also suggest considerable simplifications to other problems, for example, the flow over a blunt body. One may consider the pressure and velocity as given from the non-radiating solutions, solve only for the modifications on temperature (hence density) field, and determine the radiative heat transfer simultaneously.

In a report by Wang (1963), one may find a more detailed treatment of the present problem, including (1) the effect of changing the specific-heat ratio, (2) the thin solution for the cylindrical and spherical pistons, (3) results for negative β (see equation (8)) which apply to a higher temperature range than that presented in this paper.

2. Formulation

2.1. *Equations of motion*

The equations of motion are

$$\partial\rho/\partial t + \partial(\rho v)/\partial x = 0, \tag{1}$$

$$Dv/Dt = -\rho^{-1}\partial p/\partial x, \tag{2}$$

$$\frac{D}{Dt}\left(\frac{p/\rho}{\gamma-1}\right) + p\frac{D}{Dt}\left(\frac{1}{\rho}\right) = \frac{1}{\rho}\frac{\partial q_r}{\partial x}, \tag{3}$$

where

$$D/Dt = \partial/\partial t + v\partial/\partial x; \tag{4}$$

p is pressure, ρ density; v velocity, γ specific heat ratio, x the one-dimensional co-ordinate, t time and q_r the net radiative flux; q_r is determined by Traugott & Wang (1964)

$$q_r = q_{r+} - q_{r-}, \tag{5a}$$

$$dq_{r\pm}/d\tau = \pm\sqrt{3}\, q_{r\pm} \mp 2\pi B, \tag{5b}$$

where q_{r+} and q_{r-} are the average radiant heat fluxes along two opposite directions in a one-dimensional space, τ is the optical thickness, and B is Planck's function of black-body radiation; τ and B are respectively defined by

$$\tau = \int K\,dx, \quad B = \sigma T^4/\pi, \tag{6, 7}$$

where σ is Stefan's constant, T temperature, and K the absorption coefficient per unit volume. In general, K is a complicated function of density, temperature, composition, etc. For convenience, it is taken here to vary according to a power law

$$K = K_1 \rho^\alpha T^\beta, \tag{8}$$

where K_1, α, β are constants to be determined by best fit with available opacity data.

Substituting (6) through (8) into (5a, b) and using the perfect-gas relation, one obtains

$$\frac{\partial q_{r\pm}}{\partial x} = \pm \frac{K_1}{R^\beta} \rho^\alpha \left(\frac{p}{\rho}\right)^\beta \sqrt{3}\, q_{r\pm} \mp \frac{2\sigma K_1}{R^{\beta+4}} \rho^\alpha \left(\frac{p}{\rho}\right)^{\beta+4} \quad \text{(general)}. \tag{9a, b}$$

In the thin and thick limits, (9a, b) become

$$\frac{\partial q_r}{\partial x} = -\frac{4K_1\sigma}{R^{4+\beta}} \rho^\alpha \left(\frac{p}{\rho}\right)^{\beta+4} \quad \text{(thin)}; \tag{10a}$$

$$q_r = \frac{16}{3} \frac{\sigma}{K_1} R^{\beta-4} \rho^{-\alpha} \left(\frac{p}{\rho}\right)^{3-\beta} \frac{\partial}{\partial x}\left(\frac{p}{\rho}\right) \quad \text{(thick)}. \tag{10b}$$

It is noteworthy that no dimensional constant appears in equations (1) through (3), but there are two in (9a, b), and a different one in (10b).

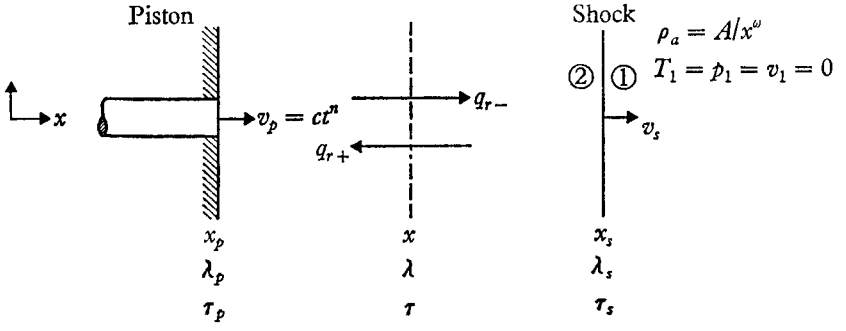

FIGURE 1. Shock generated by a moving piston.

2.2. *Boundary conditions*

We shall use the subscripts p, s, 1 and 2 as referring to the piston, shock, and the regions immediately ahead and behind the shock, respectively (figure 1). The piston moves with velocity $v_p = ct^n$; c and n are constants. For the piston location, $x_p = ct^{n+1}/(n+1)$, to increase as t increases ($t > 0$), n must be greater than -1. Ahead of the shock, the gas is at rest and its density varies according to

$$\rho_a = A/x^\omega, \tag{11}$$

where A and ω are constants. For radiation to be important, the strong shock approximation must be valid, i.e. $p_1 = T_1 = 0$. The boundary conditions to be satisfied immediately behind the shock are

$$p_2 = \{2/(\gamma+1)\}\rho_1 v_s^2, \quad \rho_2 = \{(\gamma+1)/(\gamma-1)\}\rho_1, \tag{12a, b}$$

$$v_2 = \{2/(\gamma+1)\} v_s, \quad (q_{r+})_2 = 0. \tag{12c, d}$$

Condition (12*d*) states that the gas receives no radiation from in front of the shock. Conditions (12*a*, *b*, *c*) are the usual strong-shock jump conditions. It is true that the conservation of energy across the shock should contain the radiation flux term; however, since the shock is assumed to be transparent, the radiation flux is the same on both sides, hence dropping out from the conservation of energy relation. In the thick limit, this disagrees with Elliott's work where $q_{r_1} = 0$, but $q_{r_2} \neq 0$, i.e. $q_{r_1} \neq q_{r_2}$. The boundary conditions at the piston are

$$v = v_p = ct^n, \quad (q_{r-})_p = 0. \tag{13a, b}$$

Again condition (13*b*) states that the gas receives no radiation from the piston.

For a similar flow, the shock location, x_s, must be proportional to the piston location, x_p, i.e. $x_p = \delta x_s$ where the constant δ is not known until the problem is solved. Clearly $v_p = \delta v_s$.

We have now completed the formulation of a two-sided boundary-value problem. For similarity study, it is important to notice that the above boundary conditions introduce two fundamental dimensional parameters, namely c and A.

3. Similarity considerations

3.1. *Similarity conditions*

Sedov (1959) shows that for the present type of problem, if there are only two parameters with independent dimensions, the motion is self-similar. In addition to c and A introduced through the boundary conditions, the radiative flux equations (9*a*, *b*) contain two new dimensional constants, K_1/R^β and $\sigma K_1/R^{\beta+4}$. To have a similarity solution, the dimensions of these two new constants, therefore, must be expressible in terms of the dimensions of c and A. This leads to two conditions which we shall call similarity conditions. Simple dimensional analysis shows that these two conditions are

$$\omega = -\frac{1+n(2\beta+6)}{(n+1)(1-\alpha)} \quad \text{and} \quad \omega = \frac{n(1+2\beta)+1}{(n+1)\alpha}. \tag{14a, b}$$

Constants α, β, ω, n cannot all be arbitrary. If α and β are chosen according to the best fit of a power law with known opacity data, then n and ω will be determined by (14*a*, *b*). We observe from (14*a*, *b*) that no similarity solution can be found in the present work for either the constant piston velocity case ($n = 0$) or the constant ambient density case ($\omega = 0$) if the optical thickness is arbitrary.

In the thin limit, the dimensional constant in (10*a*) is the same as one of those in (9*a*, *b*); the similarity condition is simply the one given by (14*a*). In the thick limit, the dimensional constant, $\sigma R^{\beta-4}/K_1$, in (10*b*) is obtained by dividing $\sigma K_1/R^{\beta+4}$ by $(K_1/R^\beta)^2$; hence, the corresponding similarity condition is obtained by first multiplying (14*b*) by 2α and then adding it to $(1-\alpha)$ times (14*a*); the result is

$$\omega = \{n(2\beta-4)+1\}/(n+1)(1+\alpha). \tag{15}$$

For both limiting cases, similarity solutions may be found when either $\omega = 0$ or $n = 0$.

3.3. *Similarity transformation*

We introduce

$$\lambda = x/x_s, \quad \bar{v}(\lambda) = v(x,t)\,t/x, \quad \bar{\rho}(\lambda) = \rho(x,t)/\rho_a(x), \tag{16a, b, c}$$

$$\bar{p}(\lambda) = p(x,t)\,t^2/\rho_a(x)\,x^2, \quad \bar{q}_{r\pm}(\lambda) = q_{r\pm}(x,t)\,t^3/\rho_a(x)\,x^3. \tag{16d, e}$$

Substituting equations (16*a*)–(16*e*) into (1) through (3) and (9*a*, *b*), and rearranging, yields

$$\bar{v}' = \frac{\bar{v}(\bar{v}-1)\,[\bar{v}-(n+1)] + [\{(n+1)\,(\omega-2)+2\}/\gamma - \bar{v}]\,\gamma\bar{p}/\bar{\rho}}{\lambda\{\gamma\bar{p}/\bar{\rho} - [\bar{v}-(n+1)]^2\}} + \frac{[(\gamma-1)/\bar{\rho}]\,[\lambda(\bar{q}'_{r+}-\bar{q}'_{r-}) + (3-\omega)\,(\bar{q}_{r+}-\bar{q}_{r-})]}{\lambda\{\gamma\bar{p}/\bar{\rho} - [\bar{v}-(n+1)]^2\}}, \tag{17a}$$

$$\bar{\rho}' = \bar{\rho}[(\omega-1)\,\bar{v} - \lambda\bar{v}']/\lambda[\bar{v}-(n+1)], \tag{17b}$$

$$\bar{p}' = (\bar{\rho}/\lambda)\,\{(\omega-2)\,(\bar{p}/\bar{\rho}) + \bar{v}(1-\bar{v}) - \bar{v}'\lambda[\bar{v}-(n+1)]\}, \tag{17c}$$

$$\bar{q}'_{r\pm} = \lambda^{-1}\{[(\omega-3) \pm \sqrt{3}\,c_1(\bar{\rho})^{\alpha}\,(\bar{p}/\bar{\rho})^{\beta}/\lambda^{2\beta/(n+1)}]\,\bar{q}_{r\pm} \mp 2c_2(\bar{\rho})^{\alpha}\,(\bar{p}/\bar{\rho})^{\beta+4}\lambda^{(2\beta+5)/(n+1)}\}, \tag{17d, e}$$

where the prime denotes differentiation with respect to λ, and

$$c_1 = (K_1 A^{\alpha}/R^{\beta})\,[c/\delta(n+1)]^{2\beta/(n+1)}, \tag{18a}$$

$$c_2 = (\sigma K_1 A^{\alpha-1}/R^{\beta+4})\,[c/\delta(n+1)]^{(2\beta+5)/(n+1)}. \tag{18b}$$

Substituting (16*a*)–(16*e*) into (10*a*) for the thin limit gives the expressions identical to (17*d*, *e*) with $c_1 = 0$. Substituting (16*a*)–(16*e*) into (10*b*) for the thick limit gives

$$q_r = \frac{16}{3}\frac{c_2}{c_1^2}\frac{\lambda^{(5-2\beta)/(n+1)}}{\bar{\rho}^{\alpha}}\left[\lambda\frac{d}{d\lambda}\left(\frac{\bar{p}}{\bar{\rho}}\right) + 2\frac{\bar{p}}{\bar{\rho}}\right]. \tag{19}$$

The relative magnitude of the dimensionless constants c_1 and c_2 measures the absorption property of the gas medium.

The corresponding transformed boundary conditions are:
At the shock ($\lambda = 1$), from (12*a*)–(12*d*),

$$\bar{\rho} = \bar{\rho}_2 = (\gamma+1)/(\gamma-1), \quad \bar{v} = \bar{v}_2 = 2(n+1)/(\gamma+1), \tag{20a, b}$$

$$\bar{p} = \bar{p}_2 = 2(n+1)^2/(\gamma+1), \quad \bar{q}_{r+} = (\bar{q}_{r+})_2 = 0. \tag{20c, d}$$

At the piston ($\lambda = \lambda_p$), from (13*a*) and (13*b*),

$$\bar{v} = \bar{v}_p = n+1, \quad \bar{q}_{r-} = (\bar{q}_{r-})_p = 0. \tag{21a, b}$$

The denominator of (17*a*)–(17*e*) vanishes at

$$\lambda = \bar{v} - (n+1) = \gamma\bar{p}/\bar{\rho} - [\bar{v}-(n+1)]^2 = 0;$$

however, none of these cases occur within our range of interest if the integration starts from the shock toward the piston. Condition $\bar{v}-(n+1) = 0$ occurs right at the piston, i.e. the end of integration. The equation $\gamma\bar{p}/\bar{\rho} = [\bar{v}-(n+1)]^2$ means physically that the velocity of sound is equal to the particle velocity relative to the shock velocity. It is well known that flow behind a normal shock must be subsonic, i.e. $[\bar{v}-(n+1)]^2 < \gamma\bar{p}/\bar{\rho}$.

4. Solution and result

4.1. *Exact and thin solutions*

Analytic solution of (17*a*)–(17*e*) is not believed to be feasible, so we must resort to the numerical method. Since the value of $\bar{q}_{r-}$ at the shock is not known until the problem is solved, we shall follow the standard procedure for integrating a two-sided boundary-value problem by guessing a value for $(\bar{q}_{r-})_s$ and carry on the integration step by step until $\bar{v} = \bar{v}_p$. The arbitrarily chosen value of $(\bar{q}_{r-})_s$ will not be the correct one unless the condition $(\bar{q}_{r-})_p = 0$ is satisfied.

While the exact (arbitrary opacity) solution is a two-sided boundary-value problem, the thin (transparent opacity) limit solution for a plane piston can be seen to be an initial-value one. The calculations of $\bar{v}, \bar{\rho}, \bar{p}$ are decoupled from that of $\bar{q}_r$ after the substitution of (17*d*, *e*) with $c_1 = 0$ into (17*a*), and the boundary conditions (20*a*, *b*, *c*) provide sufficient initial values at the shock. The radiation flux can be determined independently as

$$\bar{q}_r(\lambda) = -\int_\lambda^1 g_+(\eta)\left(\frac{\eta}{\lambda}\right)^{3-\omega}\frac{d\eta}{\eta} - \int_{\lambda_p}^{\lambda} g_-(\eta)\left(\frac{\eta}{\lambda}\right)^{3-\omega}\frac{d\eta}{\eta}, \tag{22}$$

where

$$g_\pm(\eta) = \mp\, 2c_2[\{\bar{\rho}(\lambda)\}^\alpha \{\bar{p}(\lambda)/\bar{\rho}(\lambda)\}^{\beta+4}\lambda^{(2\beta+5)/(n+1)}]_{\lambda=\eta}. \tag{23}$$

Clearly $\bar{q}_r(\lambda)$ can be evaluated once $\bar{\rho}(\lambda)$, $\bar{p}(\lambda)$ are known (hence, λ_p is known). The purpose of carrying out the thin solutions here along with the exact solution is twofold: first, to help make a better initial $\bar{q}_{r-}$ estimate at the shock for the exact solution; secondly, to evaluate the accuracy of the thin approximation in comparison with the exact solution.

The final distributions of the real physical variables are obtained from the similarity solutions through the relations

$$\frac{\rho}{\rho_2} = \frac{\gamma-1}{\gamma+1}\frac{\bar{\rho}}{\lambda^\omega}, \quad \frac{p}{p_2} = \frac{\gamma+1}{2(n+1)^2}\bar{p}\lambda^{2-\omega}, \tag{24a, b}$$

$$\frac{v}{v_2} = \frac{\gamma+1}{2(n+1)}\bar{v}\lambda, \quad \frac{q_r}{q_{r_2}} = \frac{\bar{q}_r}{\bar{q}_{r_2}}\lambda^{3-\omega}, \tag{24c, d}$$

which follow from (16*b*)–(16*e*) and (20*a*)–(20*d*). Values of v_2, p_2, ρ_2 are determined by (13*a*, *b*, *c*). q_{r_2} can be evaluated according to (16*e*) once $\bar{q}_{r_2}$ becomes known after the flow equations are integrated.

4.2. *Numerical integration*

The thin solutions were carried out first. The IBM program was tested by reproducing some of the known results of Kochina & Mel'nikova (1958). The IBM program for the exact solutions was tested by requiring that it reproduce the results of the thin solutions for cases where both are supposed to be valid.

The dimensionless constants, c_1, c_2, in (17*d*, *e*) depend on $c, A, \alpha, \beta, K_1, n, \sigma, R, \delta$. c and A are the fundamental dimensional parameters of our problem, representing separately the effects of the piston velocity and the ambient density. Constants α, β, K_1 are determined by fitting (9) to the opacity data of air (Wang 1963) and n and ω are determined by (14*a*, *b*); $\sigma = 5{\cdot}735 \times 10^{-5}$ erg/cm^2 sec °K,

$R = 2{\cdot}882 \times 10^6$ erg/g °K. The value of δ is not known until the problem is solved, so the actual steps run as follows: for given values of A and c/δ, one calculates c_1 and c_2 from (18a, b) and proceeds to perform the numerical integrations. When the integrations are completed, the value of $\delta = \lambda_p$ becomes known, and c is determined thereafter.

4.3. *Results and discussion*

Numerical integration has been carried out for various cases, including both positive and negative values of β, n and ω and different values of c, A, α and γ. The radiation effects were discovered to follow pretty much the same pattern. Presented in this paper is one set of such results for the case of $\alpha = 1$, $\beta = 5$, $K_1 = 0{\cdot}168 \times 10^{-17}$ cm^2/g (°K)^5, $n = -0{\cdot}0625$, $\omega = \frac{1}{3}$, $\gamma = 1{\cdot}1$, $A = 1{\cdot}29 \times 10^{-5}$ and $1{\cdot}29 \times 10^{-4}$ g/cm$^{3-\omega}$ and various c cm/sec^{n+1}. Current opacity data indicates that $\alpha = 1$ and $\beta = 5$ are valid for temperatures up to 15,000 °K.

In figure 2(a)–2(d), values of $4c_2$ rather than c are used, for convenience, as the varying parameter in labelling the curves. The case of $c_1 = c_2 = 0$ corresponds to the non-radiating solution. Deviation from the curve marked 'non-radiating' represents the radiation effect.

Figure 2(a) shows that the pressure is practically unchanged by radiation. Since all curves are so close to each other, only a few are actually plotted. The maximum change (compared to the non-radiating curve) due to radiation is about 2 % of p_2. The same is true for the velocity distribution (figure 2(b)); its maximum change due to radiation is again only 3 % of v_2. The density (hence, the temperature) and heat flux (figures 2(c) to 2(d) are, however, greatly affected; the density may be increased by over 120 % of ρ_2.

As c increases, the radiation effects become gradually prominent and the thin solutions begin to deviate from the exact ones, implying that the gas becomes optically thicker. If the parameter A is increased, the deviation between the thin solution and the exact solution becomes larger and larger. This simply says that higher ambient density causes the gas between the shock and the piston to be more opaque. Meanwhile, the density profile tends to consist of two thin boundary layers separated by a flat part. Since the pressure is not affected by the radiation, the temperature profile clearly consists of two thermal boundary layers separated by an isothermal layer. This agrees with the results of Yoshikawa & Chapman (1962) and Goulard (1963) despite the fact that their problems are steady ones. Presumably, the underlying reason responsible for this situation is that the velocity of the propagation of radiation is much larger than the flow velocity, no matter whether it is steady or unsteady.

As c_2 increases, the shock distance (distance between the shock and the piston) is gradually reduced. However, there exists a limiting value of c_2, or, equivalently, there exists a minimum shock distance; for c_2 slightly larger than this limiting value, no solution can be found, and the shock distance jumps from that minimum value to zero. The minimum shock distance for the present case is $\lambda_p \cong 0{\cdot}964$.

Values of the radiant heat flux are of particular interest in the present investigation. Detailed distributions of the net radiation flux, q_r/q_{r_2} are shown in figure 2(d) where the positive part implies $q_{r+} < q_{r-}$, i.e. the net radiant heat flows

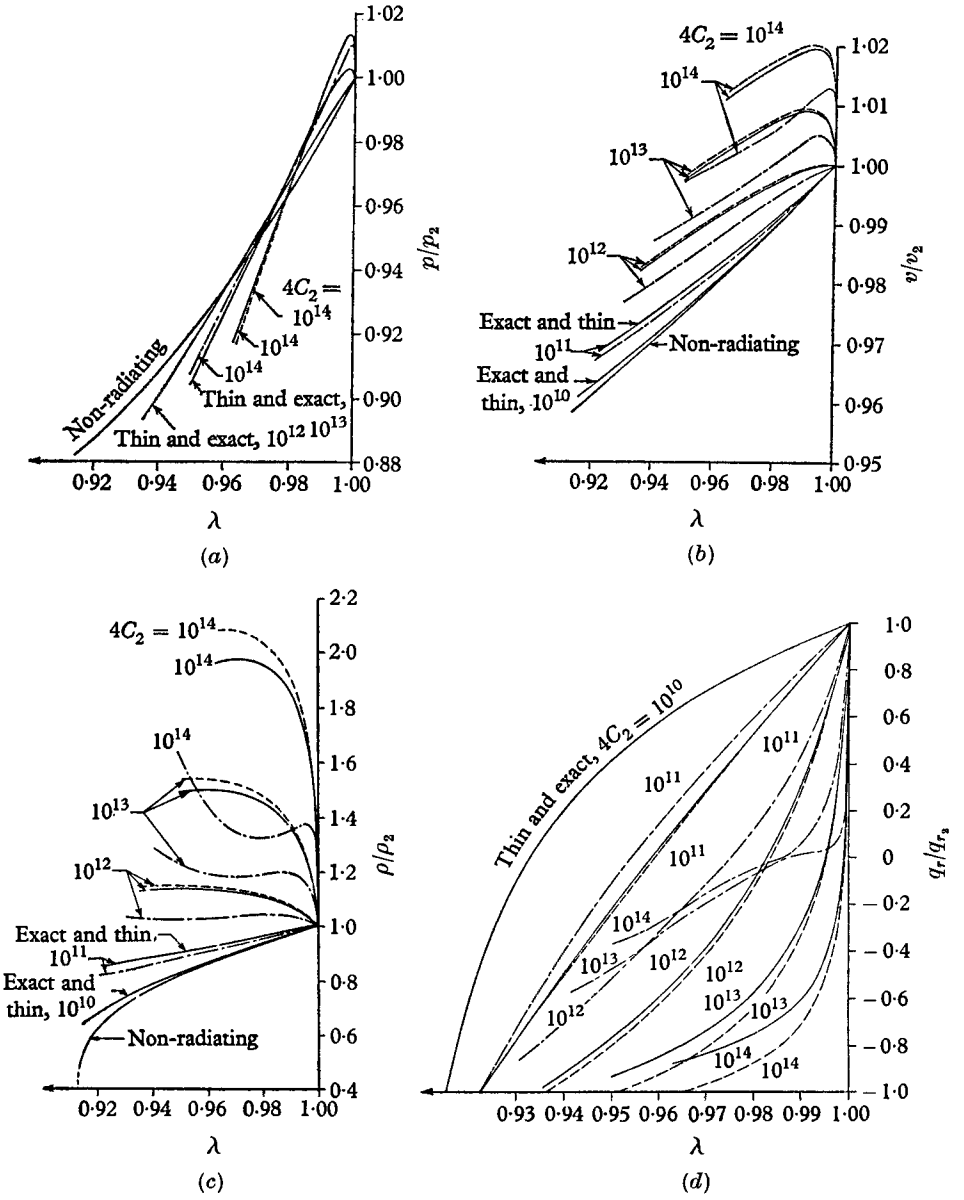

FIGURE 2. $\alpha = 1$, $\beta = 5$, $\gamma = 1{\cdot}1$; ---, thin solution; —, exact solution, $A = 1{\cdot}29 \times 10^{-5}$ g/cm$^{3-\omega}$; — · —, exact solution, $A = 1{\cdot}29 \times 10^{-4}$ g/cm$^{3-\omega}$.

(*a*) Pressure distribution.
(*b*) Velocity distribution.
(*c*) Density distribution.
(*d*) Net radiative flux distribution.

toward the shock, the negative part implies $q_{r+} > q_{r-}$, i.e. the net radiant heat flows towards the piston. Somewhere between the shock and piston, $q_{r+} = q_{r-}$, so that the net heat flux is zero. For $c_2 = 10^{10}/4$ (corresponding lower piston velocity and lower temperature behind the shock), q_r/q_{r_2} is positive over most of

the flow region. As c_2 increases up to $10^{14}/4$ corresponding to higher piston velocity and higher temperature, q_r/q_{r_2} is negative over almost the entire flow region. This is because the higher temperature region moves closer to the shock.

The thin solutions always yield equal net heat flux at the piston and at the shock (figure 2 (*d*)). This is, of course, what is expected physically. Each particle emits in both directions the same amount of energy which, in the absence of absorption, will eventually flow into the piston or pass through the shock. When the absorption is taken into consideration, the exact solutions show that the heat flux at the piston is smaller than that at the shock, i.e. $|q_{r_p}/q_{r_2}| < 1$. Again, this is because the higher temperature region moves closer to the shock.

In conclusion, we have shown, using the similarity method, that the thermal radiation practically does not affect the pressure and velocity, but decreases the temperature and hence increases the density considerably. The shock distance is reduced until a minimum value is reached. We have also demonstrated how the thin solutions deviate from the exact solutions and how a complete pattern of the radiative heat transfer varies.

The author wishes to express his gratitude to Dr S. H. Maslen for his discussions and encouragement during the course of this work, and to Mr B. Cramer for programming the numerical integration.

REFERENCES

ADRIANOV, V. N. & POLYAK, G. L. 1963 *Int. J. Heat & Mass Transf.* **6**, 355.

ELLIOTT, L. A. 1960 *Proc. Roy. Soc.* A, **258**, 287.

GOULARD, R. 1963 *AIAA* Preprint no. 63–452.

KOCHINA, N. N. & MEL'NIKOVA, N. S. 1958 *Prik. Mat. Mek.* **22**, 622.

KOROBEINIKOV, V. P. 1957 *Dokl. Akad. Nauk, U.S.S.R.*, **113**, 1006.

MARSHAK, R. E. 1958 *Phys. Fluids*, **1**, 24.

SEDOV, L. I. 1959 *Similarity and Dimensional Methods in Mechanics*, p. 146. New York: Academic Press.

TAYLOR, G. I. 1946 *Proc. Roy. Soc.* A, **186**, 273.

TRAUGOTT, S. C. & WANG, K. C. 1964 *Int. J. Heat & Mass Transf.* **7**, 2, 269.

TRILLING, L. 1963 *IAS* Preprint no. 63–54.

YOSHIKAWA, K. K. & CHAPMAN, D. R. 1962 *NASA* TN-D-1424.

WANG, K. C. 1963 *Martin Company Research Report* RR-47.